Report on a problem studied at the UK Mathematics-in-Medicine Study Group Southampton 2007
< https://mmsg.mathmos.net/uk/2007/blood-pressure/ >

7TH Mathematics in Medicine Study Group
University of Southampton, 10–14 September 2007

Continuous Non-Invasive Blood-Pressure Measurements

Problem presented by
Dr. Tony Birch
Neurological Physics Group, Southampton University Hospital Trust

	Chris Breward	Sarah Campbell	Igor Chernyavsky
	Thorsten Fischer	Steven Glavin	Oliver Jensen
Participants:	Anna Lovrics	Sarah McBurnie	Jonathan Moles
	Colin Please	Jennifer Siggers	Peter Stewart
	Christopher Voyce	Robert Whittaker	Tom Witelski

Summary Presentation (14 Sept 2007)
Report coordinator Robert Whittaker
(Report: [18 October 2007] version)

1 Introduction

1.1 The Problem Presented to the Study Group

The primary components of healthy living are recognised as a good diet, plenty of exercise, avoiding smoking and reducing stress. These measures are largely aimed at improving the health of the arterial system. The arterial system is much more than a set of pipes, it is an extraordinarily well-regulated blood delivery network capable of responding within a few seconds to challenges such as an altered body position, or a change in demand. There is rapidly growing interest in measurement techniques that can assess the rapid dynamics of the arterial system. These may enable deteriorating function to be identified before it becomes problematic. Much of the research in this area requires a continuous but non-invasive measure of arterial pressure.

Arterial blood pressure may be measured continuously by two different non-invasive techniques; the Finapres™ and Colin® CBM-7000 Radial Artery Tonometer, both described below. The Study Group was asked to explore explanations for the disagreement in output of the two techniques. In particular, by modelling the behaviour of both devices and their vascular response to the provocation.

1.2 Description of the Finapres

We first describe the Finapres, which uses infrared light transmission to measure arterial pressure in the finger (Penaz, 1973; Wesseling *et al.*, 1995; Imholz *et al.*, 1998). Since the wavelength of light used is primarily absorbed by haemoglobin, monitoring light intensity fluctuations transmitted through the finger provides information about the area of the finger cross section occupied by blood. The volume of the blood is related to pressure (see Langewouters *et al.*, 1986;

(a)

(b)

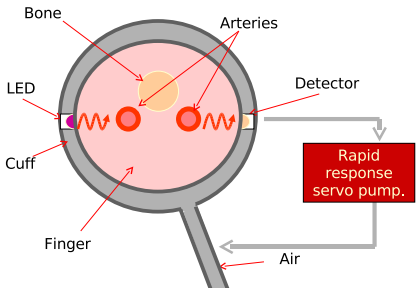

FIGURE 1: *The Finapres. (a) A photograph showing the cuff placed under a finger. During operation the cuff is wrapped firmly around the finger and held in place by velcro. (b) A cross-section of the finger showing how the Finapres operates.*

Drzewiecki *et al.*, 1996) , and so we are in fact able to track blood pressure changes. It is this principle that is exploited by the Finapres.

The Finapres, shown in figure 1, uses a cuff around a finger that can apply a varying pressure. The applied cuff pressure p_{ext} is varied in time so that the light intensity is maintained at a constant value. If the light intensity increases, this indicates a drop in blood volume within the cuff. In response, the cuff pressure is reduced to allow more blood to flow, and hence the light intensity decreases back to the target value. The cuff pressure applied to do this is related to the blood pressure.

After securing the cuff around the patient's finger, the Finapress calibrates itself as follows:

1. The cuff is inflated to some minimum pressure p_{ext}, below normal blood pressure.
2. The light intensity $I(t)$ is measured over several blood pulses, and the amplitude of the oscillations in $I(t)$ is recorded.
3. The cuff pressure p_{ext} is increased in small increments, and step 2 is repeated for each value of p_{ext}.
4. The cuff pressure that maximises the amplitude of the oscillations in light intensity is found, and recorded as p^*_{ext}.
5. Holding the cuff at fixed pressure p^*_{ext}, the mean light intensity over several heart cycles is recorded as I^*.

This completes the calibration procedure. The device now dynamically varies p_{ext} in order to keep the light intensity fixed at I^*. The value of p_{ext} is output as the patient's blood pressure.

The calibration procedure is designed to make the apparatus as sensitive as possible to light changes, and hence to detecting pressure changes. Crucially, it is also hoped that the calibration is such that the cuff pressure applied is equivalent to the blood pressure itself. This assumption is a possible source of error, and one aim of the study is to investigate the relationship between the blood pressure and the cuff pressure, through mathematical modelling.

1.3 Description of the Tonometer

The Colin CBM-7000 tonometer estimates the pressure in the radial artery at the wrist, see for example Kemmotsu *et al.* (1991); Sato *et al.* (1993); Weiss *et al.* (1996). A line of piezoelectric crystals lying perpendicular to the axis of the artery is then pressed against the skin over the radial artery. These are held in place with a constant force, and the oscillations in their position

(a)

(b)

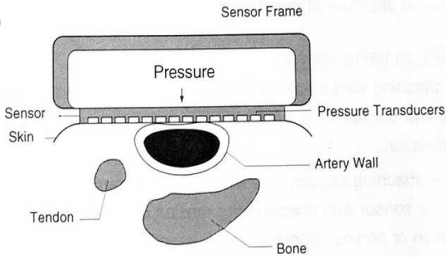

FIGURE 2: *The Colin Radial Artery Tonometer. (a) A photograph of the device in operation. The pressure transducers are located in the central block, and the straps at either end are part of a separate splint designed to keep the wrist still. (b) A cross-section of the wrist showing how the device works.*

are measured. A photograph of the device in operation and a sketch showing a cross-section of the wrist are shown in figure 2.

A separate oscillometric cuff over the upper arm is used to find the systolic and diastolic arterial pressures at the start of the measuring period. These maximum and minimum values are then used to calibrate the continuous pressure readings from the tonometer.

Therefore the actual readings from the transducers are not important, as long as they can be mapped (presumably linearly) on to the pressure scale. The tonometer can be set to periodically re-calibrate itself using the cuff. However, in the experiments considered in this study, the re-calibration feature was deliberately deactivated.

1.4 Discrepancies in experiments

Two experiments have exposed differences in the measurement of the two devices. The first of the experiments is reported by Birch & Morris (2003). A cuff was placed around the patients' thighs and left for 3 minutes 20 seconds. Due to vasodilation, this caused the vessels in the legs to dilate in order to try to increase blood flow there. Finapres and Tonometer readings were taken continuously and simultaneously. The thigh cuffs were rapidly deflated and pressure readings taken for approximately thirty seconds subsequently. After cuff deflation, the leg vessels filled with blood, venous return and cardiac output fell, and the upper body arterial pressure dropped. After approximately ten seconds, the pressure began to return to its normal value, as shown in figure 3.

The second of the experiments involved enclosing the lower half of the body in a pressure chamber and applying a negative pressure that varied sinusoidally with time.[1] Birch (2007) describes the different readings that were recorded by the two devices, as shown in figure 4.

It is not known for either experiment which (if either) of the two readings is correct, nor what the reason is for the discrepancy. One of the aims of this work therefore, is to lay the foundation for models that may be used to test possible explanations. There are a few obvious possibilities:

- In both cases the Finapres readings fall lower than those of the Tonometer during a period of induced low pressure. This may be because the blood pressures differ between the arteries, leaving the possibility that both readings are correct. When the body is put under stress due to low blood pressure, the peripheral vessels vasoconstrict in order to restrict blood supply. The aim of the body is to increase blood pressure elsewhere, in

[1] This technique has previously been used for other purposes, e.g. Birch *et al.* (2002).

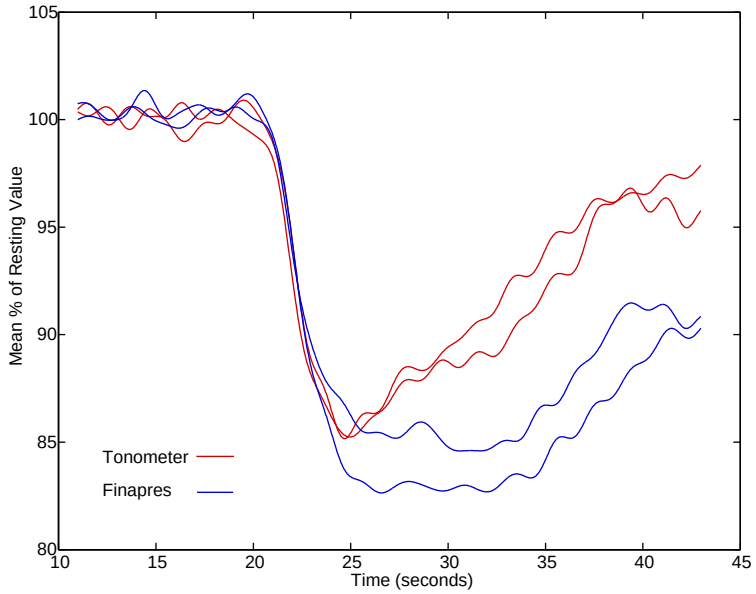

FIGURE 3: *Average blood-pressure measurements from the tonometer and Finapres for the leg-cuff experiments of Birch & Morris (2003).* © *IOP Publishing.*

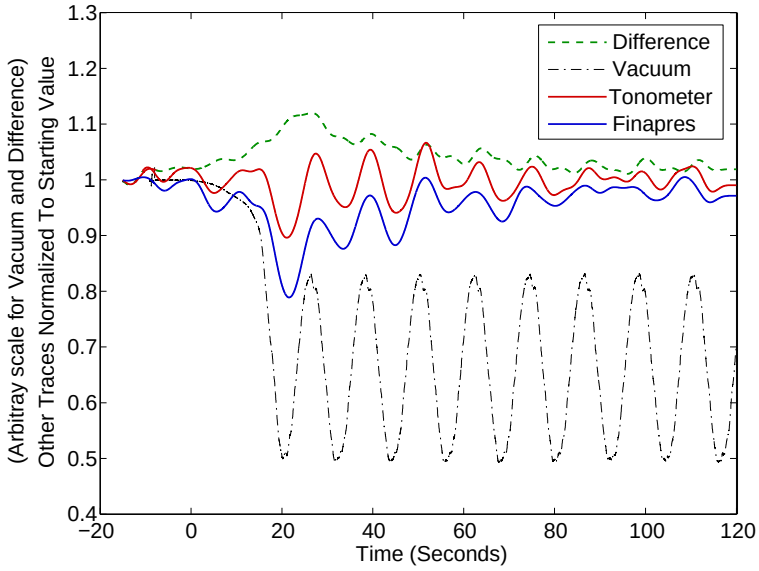

FIGURE 4: *Average blood-pressure measurements from the tonometer and Finapres for the lower-body pressure chamber experiments of Birch (2007).* © *Lippincott Williams & Wilkins.*

particular in the vital organs, at the expense of the less-important periphery. This may account for a lower pressure in the finger artery.

- The Finapres measurement assumes that the cuff pressure needed to maintain light intensity equals the arterial blood pressure. There are several possible reasons why this assumption may be incorrect:
  - The cuff pressure may not be uniformly transmitted through the finger, and so the effective pressure on the artery caused by the cuff may not equal the cuff pressure.
  - The cuff pressure at which the maximum amplitude of variation in transmitted light is observed may not equal the mean arterial pressure.
  - The Finapres works on the assumption that the only blood under the cuff is in the artery, since the vein and other vessels will be closed due to their lower pressures. However, blood continues to pass through the artery during Finapres use, leading to an increase in blood volume in the capillaries at the end of the finger. Consequently the pressure there begins to rise. Eventually the venous pressure will become comparable with arterial pressure, at which point blood will flow back along the vein. This flow and its implications for the Finapres readings are not well understood.
- For the tonometer:
  - The initial calibration is done using an oscillometric cuff, which has errors of up to approximately 15% (O'Brien *et al.*, 2001). Thus, however accurately subsequent readings are taken, the accuracy of the Tonometer output is limited.
  - The Tonometer manual does not describe how it uses the pressures found during calibration to interpolate its readings from the crystal and hence calculate the time-dependent pressures (the simplest way would be linear interpolation). It may be that the interpolation used is not well-justified. Moreover, if the range of pressures during the cycle changes significantly, assumed interpolation may not extend well outside the initial range.
  - Physiological changes (e.g. a stiffening of the arterial wall) may mean that a certain arterial pressure gives a different transducer signal at a later time than it did initially.

It is also not well understood how inter-patient variations affect the readings. In particular, the distribution and type of fat and muscle in the patient would seem to be important for both devices. For the Tonometer it would affect the elastic properties of the wrist flesh, whilst for the Finapres the effect on the transmitted light intensity is difficult to interpret. Many patients are elderly, and another important factor to consider is the effect of arterial stiffness, which tends to increase with age. If the stiffness affects the accuracy of either reading, it may have important implications.

2 Tonometer Models

In this section, we develop two models for the tonometer behaviour; a simple spring-and-dashpot model, and a more advanced viscoelastic slab model. Our objective here is to determine whether or not the tonometer is likely to give a true measure of blood pressure. We do this by constructing a mechanical model and comparing the input (the true blood pressure) with the output (the blood pressure as measured by the tonometer). Further, we ask whether or not the readings given by the tonometer model are sensitive to changes in the strength of the arterial walls.

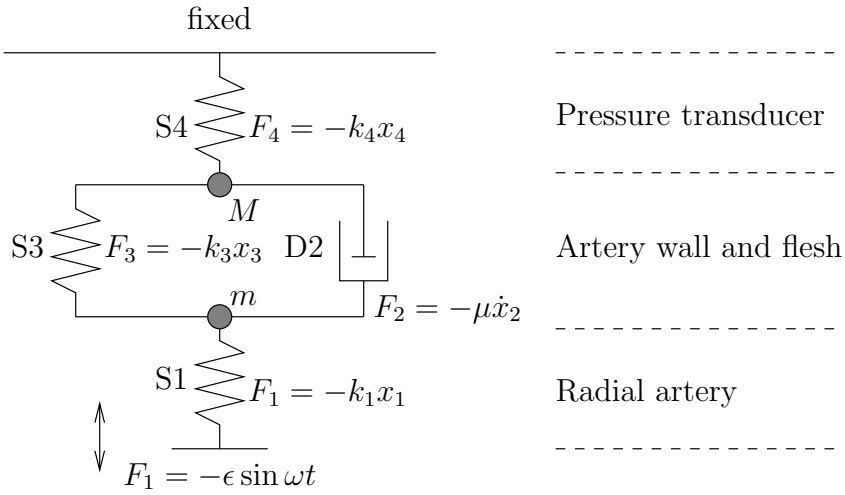

FIGURE 5: *A schematic of the spring-and-dashpot model of the radial artery tonometer that is described in §2.1.*

2.1 Spring-and-dashpot model

We first consider a simple spring-and-dashpot system to mimic the constituent blood, artery wall and tissue components of the biological system. A schematic of the model is shown in figure 5.

We consider motion between two rigid plates, where the upper plate represents the meter that measures the pressure and the lower plate is moved in order to apply a pressure to the vessel wall above. The upper plate is fixed in space and we prescribe oscillations of the lower plate about its equilibrium position such that we obtain a given force $F_1 = -\epsilon \sin(\omega t)$ in the spring (S1) representing the pulsating blood pressure. The wall of the radial artery expands in response, and the tissue between the wall of the artery and the tonometer deforms and dissipates energy. The wall and tissue are modelled as a spring (S2) and dashpot (D3) placed in parallel. The spring constant k_3 depends on time to model the changing stiffness of the artery wall. The pressure transducers are modelled as a spring (S4) with a high spring constant k_4.

The governing equations are obtained by balancing forces at each mass-point, giving

$$m\left(\frac{\mathrm{d}^2 x_4}{\mathrm{d}t^2} + \frac{\mathrm{d}^2 x_2}{\mathrm{d}t^2}\right) = -\mu \frac{\mathrm{d}x_2}{\mathrm{d}t} - k_3 x_3 + k_1 x_1 \,, \tag{1}$$

$$M\frac{\mathrm{d}^2 x_4}{\mathrm{d}t^2} = -k_4 x_4 + k_3 x_3 + \mu \frac{\mathrm{d}x_2}{\mathrm{d}t} \,. \tag{2}$$

We also have that $x_2 = x_3$ from the parallel configuration, and that the forcing is given by

$$k_1 x_1 = \epsilon \sin(\omega t) \,. \tag{3}$$

The initial conditions at $t = 0$ are chosen, for simplicity, to be

$$x_2 = 0 \,, \qquad x_4 = 0 \,, \qquad \frac{\mathrm{d}x_2}{\mathrm{d}t} = 0 \,, \qquad \frac{\mathrm{d}x_4}{\mathrm{d}t} = 0 \,, \tag{4}$$

and the parameter values assumed are given in table 1. To model the effect of a stiffening artery wall, we also consider using a time-dependent spring constant for S3:

$$k_3 = \frac{1}{2}\left[1 + \tanh\left(\frac{t - t_0}{\Delta T}\right)\right](k_{31} - k_{30}) + k_{30} \,. \tag{5}$$

Parameter	Symbol	Typical Value
Forcing frequency	ω	0.5
Forcing amplitude	ϵ	0.2
Lower mass	m	1
Upper mass	M	2
D2 Damping coefficient	μ	1
S1 Spring constant	k_1	1
S3 Spring constant	k_{30}	1
S3 Spring constant	k_{31}	10
S4 Spring constant	k_4	5×10^3
Stiffening time	t_0	0
Stiffening timescale	ΔT	2

TABLE 1: *Dimensionless parameter values used in the spring-and-dashpot tonometer model of §2.1.*

The system (1)–(4) was solved numerically using standard library routines. The results indicated that, after an initial period of transient behaviour (induced by the choice of boundary conditions), the tonometer readings compare well with the real blood pressure. Figure 6 shows the transient behaviour and transition to a periodic oscillatory state, with k_3 as defined in (5), and the parameters given in table 1.

It is observed that when k_4 is large, the response of the tonometer is insensitive to the choice of k_3, even if k_3 varies with time. This is an important finding, since it confirms that the tonometer is likely to be an equally accurate method of blood pressure measurement in a wide variety of patient types.

It is further observed that the time for the system to settle to a steady-state after a change in blood pressure depends on the parameter values chosen. Since the parameter values remain largely unknown, it is not possible to comment on how long the tonometer might take to accurately respond to changes in blood pressure.

We conclude that the tonometer is likely to be an accurate device for measuring blood pressure, but that a two-dimensional elastic with a prescribed force along the bottom surface would be a more accurate model.

2.2 Linear Visco-Elastic Slab

As an improvement over the previous spring-and-dashpot model, we model the skin, artery wall, and other tissue between the radial artery and the tonometer as a single uniform slab of visco-elastic material, with depth h and infinite extent horizontally. We consider a strictly two-dimensional problem in which all variables are uniform in the y direction, and take the upper and lower boundaries to be the planes $z = h$ and $z = 0$. See figure 7.

The blood pressure in the artery is denoted $p(t)$ and the width of the squashed artery in contact with the visco-elastic layer is $2a$. We assume that the normal stress on the upper surface is the pressure that is read by the tonometer. The displacement field is given by $\boldsymbol{u}$, so the strain tensor is

$$e_{ij} = \frac{1}{2}\left(\frac{\partial u_i}{\partial x_j} + \frac{\partial u_j}{\partial x_i}\right) . \tag{6}$$

We assume that the material behaves linearly, and use a Kelvin–Voigt model, whereby the

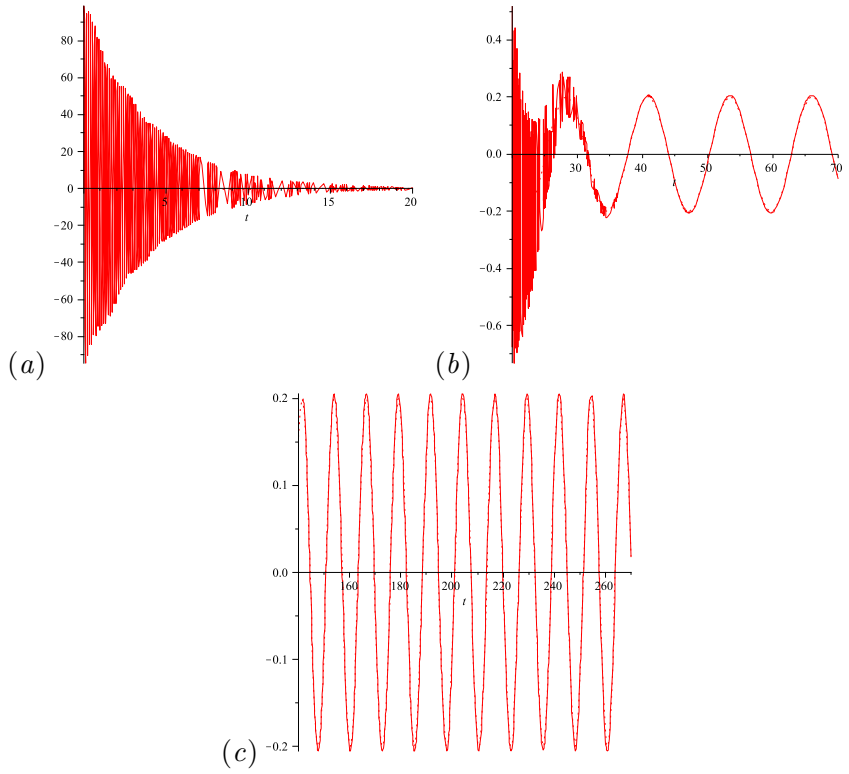

FIGURE 6: *Graphs to compare blood pressure with tonometer response for the spring-and-dashpot model. (a) Transient behaviour. (b) Transition to periodic behaviour. (c) Periodic sinusoidal behaviour.*

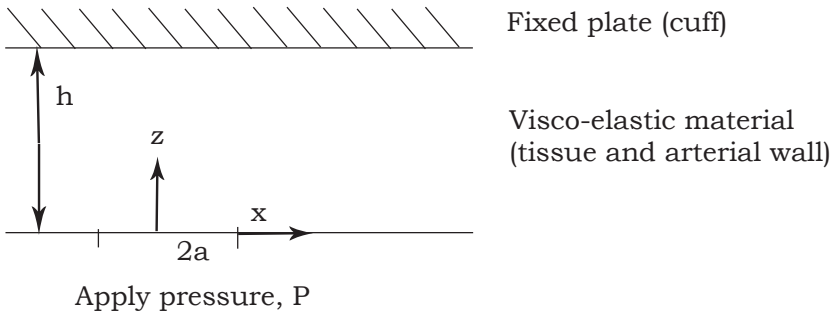

FIGURE 7: *A sketch of the geometry for linear visco-elastic tonometer model.*

stress tensor σ is the sum of separate elastic and viscous components. We therefore write

$$\sigma_{ij} = \left(\lambda e_{kk}\delta_{ij} + 2\mu e_{ij}\right) + 2\eta\left(-\frac{1}{3}\frac{\partial e_{kk}}{\partial t}\delta_{ij} + \frac{\partial e_{ij}}{\partial t}\right), \tag{7}$$

where λ and μ are the Lamé moduli from linear elasticity, and η is the Newtonian viscosity.

The momentum equation is then given in the usual way by relating the rate of change of inertia to the divergence of the stress:

$$\rho\frac{\partial^2 u_j}{\partial t^2} = \frac{\partial \sigma_{ij}}{\partial x_i} \tag{8}$$

This leads to the equation

$$\rho\ddot{\boldsymbol{u}} = (\lambda+\mu)\boldsymbol{\nabla}(\boldsymbol{\nabla}\cdot\boldsymbol{u}) + \mu\nabla^2\boldsymbol{u} - \frac{1}{3}\eta\boldsymbol{\nabla}(\boldsymbol{\nabla}\cdot\dot{\boldsymbol{u}}) + \eta\nabla^2\dot{\boldsymbol{u}}\,, \tag{9}$$

where dots are used to denote time derivatives.

We apply a rigid boundary condition on the upper boundary, since the tonometer is pressed onto the skin there, and motion of the pressure transducers is minimal. Hence

$$\boldsymbol{u} = \boldsymbol{0} \quad \text{on } z = h. \tag{10}$$

At the lower boundary we assume that the artery exerts a uniform (but temporally varying) pressure $p(t)$ over the contact area of width $2a$. Away from the artery the lower surface is stress-free. We therefore have:

$$\sigma\cdot\hat{\boldsymbol{z}} = \begin{cases} p(t)\hat{\boldsymbol{z}} & : \quad |x| < a \\ \boldsymbol{0} & : \quad |x| > a \end{cases} \tag{11}$$

The equations are linear in $\boldsymbol{u} = u\hat{\boldsymbol{x}} + w\hat{\boldsymbol{z}}$, and we solve them by taking the double Fourier transform with respect to x and t. (The conjugate transform variables are k and ω respectively.) This leaves a pair of coupled second-order ordinary differential equations in z for the transformed variables $\tilde{u}(k,z,\omega)$ and $\tilde{w}(k,z,\omega)$. These are readily solved, but it would appear that the inverse transforms can only be computed numerically. Nevertheless, it should prove instructive to examine the transform solutions, to see how the layer depth h, and visco-elastic parameters λ, μ, and η, affect the solution.

Two relevant limits that will result in simpler (but still non-trivial) problems to solve are:

1. The limit $a/h \to 0$. In this case, the lower boundary condition reduces to a point force, with
$$\sigma\cdot\hat{\boldsymbol{z}} = 2a\,p(t)\,\delta(x)\,\hat{\boldsymbol{z}} \quad \text{on } z = 0 \tag{12}$$

2. The limit $\omega^2\rho \ll \max\{\lambda,\mu,\omega\eta\}$. Then the inertial term $\rho\ddot{\boldsymbol{u}}$ may be neglected. This corresponds to the induced motions being much smaller than the speed of internal waves in the visco-elastic layer.

3 Finapres Models

3.1 Cuffed Artery Model

To model the Finapres, we first consider the simple situation depicted in figure 8(a). The blood enters through the artery, and, after filtering through a system of capillaries, exits via a vein. The Finapres cuff surrounds the artery and vein, exerting pressure on both. As explained

FIGURE 8: *(a) An idealised sketch of the Finapres and artery system. (b) A simplified system, replacing the capillaries with a jump condition. The Finapres exerts compression on both the vein and the artery.*

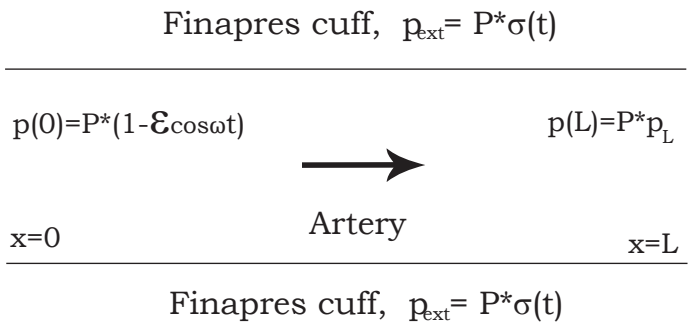

FIGURE 9: *A sketch of the highly simplified cuff–artery system modelled, and non-dimensionalised pressures and stresses.*

previously, it uses a system involving varying the pressure in order to keep the intensity of light transmission constant.

This system is simplified both by removing the capillaries and by considering just the vein and the artery. This is illustrated in figure 8(b). The capillaries in this case are replaced by a "jump condition" in the pressure.

As a first attempt to understand the workings of the Finapres, we simplify the system even further and consider the situation where there is an artery only, as shown in figure 9.

The flexible tube has length L, internal pressure $p(x)$ and an external pressure p_{ext} applied by the cuff. The upstream pressure maintained by the heartbeat provides the upstream boundary condition

$$p(0) = P^*(1 - \epsilon \cos \omega t)\,, \tag{13}$$

and we assume a constant downstream pressure

$$p(L) = P^* p_L \tag{14}$$

The varying external pressure applied by the cuff is written as

$$p_{\text{ext}} = P^* \sigma(t)\,. \tag{15}$$

We derive a simple set of governing equations for $p(x)$ as follows, by introducing the cross-sectional area $A(x,t)$ of the tube and the volume flux $Q(x,t)$ of blood.

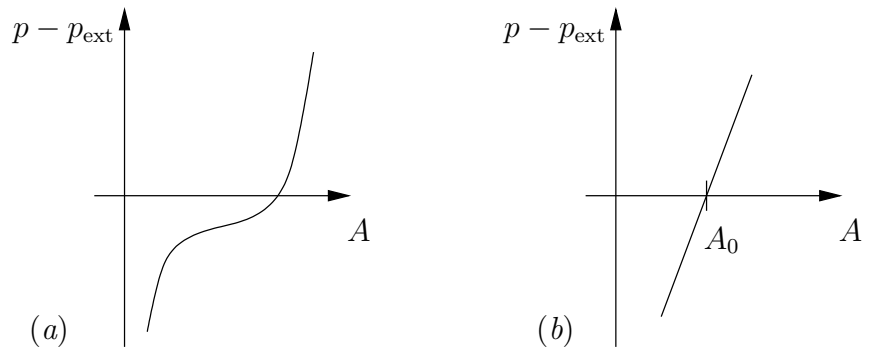

FIGURE 10: *Tube laws linking the transmural pressure $p - p_{\text{ext}}$ to the cross-sectional area A of a tube. (a) Typical behaviour of an elastic artery (see, e.g. Langewouters* et al.*, 1986). (b) The idealised linear tube law (18) used in the simple Finapres model.*

Conservation of mass yields

$$\frac{\partial A}{\partial t} + \frac{\partial Q}{\partial x} = 0\,. \tag{16}$$

Assuming viscous drag dominates inertial effects (i.e. the Reynolds number is small), Poiseuille flow in a circular tube gives

$$Q = -\frac{A^2}{8\pi\mu}\frac{\partial p}{\partial x}\,. \tag{17}$$

In this simple model we neglect errors caused by deviations from a circular cross-section.

A 'tube law' is used to describe the relationship between the cross-sectional area, and the pressure difference across the tube walls (see figure 10). We take the simple linear expression

$$A = A_0 + k(p - p_{\text{ext}})\,. \tag{18}$$

Observe that k^{-1} is a measure of the stiffness of the tube wall. As $k \to 0$ the wall stiffens so that large pressure changes are required to obtain any significant change in area.

Finally, the Finapres operates by varying p_{ext} to keep the light intensity I constant. We assume that this equates to keeping the artery at a constant volume V, i.e.

$$\int_0^L A(x,t)\,\mathrm{d}x = V\,. \tag{19}$$

To reduce the number of parameters, we non-dimensionalise the equations. We scale lengths with L and time with ω^{-1}, writing

$$x = L\xi\,, \quad \text{and} \quad t = \omega^{-1}\tau\,. \tag{20}$$

We scale pressure with the average upstream pressure P^*, and also introduce a non-dimensional transmural pressure difference

$$\theta(\xi,\tau) = \frac{p - p_{\text{ext}}}{P^*} = \frac{p}{P^*} - \sigma\,. \tag{21}$$

After non-dimensionalising, we get:

$$\frac{\partial\theta}{\partial\tau} = \mathscr{D}\frac{\partial}{\partial\xi}\left((1+\mathscr{K}\theta)^2\frac{\partial\theta}{\partial\xi}\right)\,, \tag{22}$$

Parameter	Symbol	Typical Value
Young's modulus	E	$10^4 - 10^6\,\mathrm{N\,m^{-2}}$
Wall thickness	h	$0.5 \times 10^{-3}\,\mathrm{m}$
Mean arterial radius	a	$3 \times 10^{-3}\,\mathrm{m}$
Blood density	ρ	$1 \times 10^3\,\mathrm{kg\,m^{-3}}$
Blood viscosity	ν	$4 \times 10^{-6}\,\mathrm{m^2\,s^{-1}}$
Mean blood velocity	U	$1.5 \times 10^{-1}\,\mathrm{m\,s^{-1}}$

TABLE 2: *Parameters values used in the cuffed finger artery model. (Arterial properties from Langewouters* et al. *1986.)*

$$\int_0^1 \theta \,\mathrm{d}x = \mathscr{V}\,, \tag{23}$$

where

$$\mathscr{K} = \frac{kP^*}{A_0}\,, \tag{24}$$

$$\mathscr{D} = \frac{A_0^2}{8\pi\mu k L^2 \omega}\,, \tag{25}$$

$$\mathscr{V} = \frac{1}{P^* k}\left(\frac{V}{L} - A_0\right)\,. \tag{26}$$

The boundary conditions are:

$$\theta(0,\tau) = 1 - \epsilon\cos\tau - \sigma(\tau)\,, \tag{27}$$

$$\theta(1,\tau) = p_L - \sigma(\tau)\,. \tag{28}$$

For a well-posed problem, we also require an initial condition, i.e. $\theta(\xi, 0)$.

We now go on to consider wavelength estimation in §3.2, before solving the model, with series expansions in §3.3 and §3.4, and numerically in §3.5.

3.2 Wavelength estimation

In order to estimate the characteristic wavelength of a pressure pulse wave, we refer to the Moens–Korteweg velocity c_0, which describes propagation of linear waves in a compliant tube filled with inviscid liquid (see Fung, 1993). This velocity is given by

$$c_0 = \sqrt{\frac{E\,h}{2\,a\,\rho}}\,, \tag{29}$$

where E is the Young modulus of elasticity, h is the wall thickness, a is the reference arterial radius, and ρ is the density of the blood.

Table 2 gives typical parameter values for the digital arteries. From these values, and assuming a cuff length of $L = 0.02\,\mathrm{m}$, we estimate the Reynolds number as $Re = aU/\nu = 112.5$, and the Womersley number as $\alpha = a/\sqrt{\nu T} = 1.5$. Our model for the Finapres device assumes that the aspect ratio ($a/L \sim 0.1$) of the arterial segment is small enough to neglect the inertial effects of the fluid.

Based on the data from table 2, we estimate the pulse wave velocity (29) as $c_0 \approx 1\,\mathrm{m\,s^{-1}}$. The typical period of pulse wave is $T \approx 1\,\mathrm{s}$. Thus the length of the wave is about $\Lambda \approx 1\,\mathrm{m}$, which is much bigger than the length L of the cuff.

Taking advantage of the small parameter $\varepsilon = L/\Lambda$, it is possible to introduce a slowly-varying spatial variable $X = \varepsilon\,\xi$. After completing the change of variables in (22) and the integral constraint (23), we obtain

$$\frac{\partial\theta}{\partial\tau} = \varepsilon^2\mathscr{D}\frac{\partial}{\partial X}\left((1+\mathscr{K}\theta)^2\frac{\partial\theta}{\partial X}\right), \tag{30}$$

$$\mathscr{V} = \frac{1}{\varepsilon}\int_0^{\varepsilon}\theta\,\mathrm{d}X \simeq \theta(0,t) + \frac{\varepsilon}{2}\frac{\partial\theta(0,t)}{\partial X}. \tag{31}$$

We conclude that $\theta = const \approx \mathscr{V}$, correct to $O(\varepsilon)$.

3.3 Expansion for $\epsilon \ll 1$

We begin by considering the case $\epsilon \ll 1$, and postulating a series expansion. We use the standard technique of working with a complex version of the problem, where the physical solution is taken to be just the real part of each of the variables. Accordingly the boundary condition (27) is rewritten as

$$\theta(0,\tau) = 1 - \epsilon\mathrm{e}^{\mathrm{i}\tau} - \sigma(\tau). \tag{32}$$

For simplicity, we take $p_L = 0$ in the other boundary condition, so

$$\theta(1,\tau) = -\sigma(\tau). \tag{33}$$

We then adopt the following ansatz for the leading and first-order terms:

$$\theta(\xi,\tau) = \bar{\theta}(\xi) + \epsilon\theta'(\xi)\mathrm{e}^{\mathrm{i}\tau} + O(\epsilon^2), \tag{34}$$

$$\sigma(\tau) = \bar{\sigma} + \epsilon\sigma'\mathrm{e}^{\mathrm{i}\tau} + O(\epsilon^2). \tag{35}$$

We substitute these expressions into the governing equation (22), integral constraint (23) and boundary conditions (32)–(33). At leading order in ϵ we obtain

$$\mathscr{D}\frac{\partial}{\partial\xi}\left[(1+\mathscr{K}\bar{\theta})^2\frac{\partial\bar{\theta}}{\partial\xi}\right] = 0, \tag{36}$$

$$\int_0^1\bar{\theta}(\xi)\,\mathrm{d}\xi = \mathscr{V}, \tag{37}$$

$$\bar{\theta}(0) = \mathscr{K}(1-\bar{\sigma}) + 1, \tag{38}$$

$$\bar{\theta}(1) = -\mathscr{K}\bar{\sigma} + 1. \tag{39}$$

The general solution to (36) can be written as

$$\bar{\theta}(\xi) = \frac{1}{\mathscr{K}}\left[\left(A^3\xi + B^3(1-\xi)\right)^{1/3} - 1\right], \tag{40}$$

where A and B are arbitrary constants. The boundary and integral conditions then imply

$$A = -\mathscr{K}\bar{\sigma} + 1, \tag{41}$$

$$B = \mathscr{K}(1-\bar{\sigma}) + 1, \tag{42}$$

$$\mathscr{K}\mathscr{V} = \frac{3(A^4 - B^4)}{4(A^3 - B^3)} - 1. \tag{43}$$

These three equations are sufficient to solve for the three unknowns A, B, and $\bar{\sigma}$. Eliminating A and B (and cancelling a factor of $A-B$) we obtain a cubic equation for $\bar{\sigma}$. In principle, this is soluble, and hence we can recover the complete solution.

Turning now to the $O(\epsilon)$ terms, we have

$$\mathrm{i}\theta' = \mathscr{D}\frac{\partial}{\partial\xi}\left[(1+\mathscr{K}\bar{\theta})^2\frac{\partial\theta'}{\partial\xi} + 2(1+\mathscr{K}\bar{\theta})\mathscr{K}\theta'\frac{\partial\bar{\theta}}{\partial\xi}\right], \tag{44}$$

$$\int_0^1 \theta'(\xi)\,\mathrm{d}\xi = 0\,, \tag{45}$$

$$\theta'(0) = -1-\mathscr{K}\sigma'\,, \tag{46}$$

$$\theta'(1) = -\mathscr{K}\sigma'\,. \tag{47}$$

The governing equation (44) contains a perfect derivative and can be re-written as

$$\mathrm{i}\theta' = \mathscr{D}\frac{\partial^2}{\partial\xi^2}\Big[(1+\mathscr{K}\bar{\theta})^2\theta'\Big]\,. \tag{48}$$

We now make a double substitution to transform the equation to a standard form. We introduce

$$X = (1+\mathscr{K}\bar{\theta})^2 \quad \text{and} \quad Y = \theta' X^{1/4}\,. \tag{49}$$

It may be checked from (40) that

$$\frac{\partial X}{\partial\xi} = 2(1+\mathscr{K})\mathscr{K}\frac{\partial\bar{\theta}}{\partial\xi} = \frac{2(A^3-B^3)}{3X^{1/2}}\,. \tag{50}$$

On making the substitution we obtain

$$X^2\frac{\partial^2 Y}{\partial X^2} + X\frac{\partial Y}{\partial X} - (\lambda^2X^2+\nu^2)Y = 0\,, \tag{51}$$

where

$$\nu = \frac{3}{4}\,, \qquad \lambda = \frac{3(1+\mathrm{i})}{2\sqrt{2\mathscr{D}}(A^3-B^3)}\,. \tag{52}$$

This is a modified Bessel equation, and hence we have the general solution

$$Y(X) = C\,\mathrm{I}_\nu(\lambda X) + D\,\mathrm{K}_\nu(\lambda X)\,, \tag{53}$$

where C and D are arbitrary constants, and I_ν and K_ν are modified Bessel functions of the first and second kind respectively.

One can now apply the integral and boundary conditions (45)–(47), in order to determine the three unknowns C, D, and σ'. The resulting system of equations is not particularly pleasant, and an analytical solution is unlikely, except in special cases.

3.4 Expansion for $\epsilon \ll 1$ and $\mathscr{K} = 0$

Since the $\epsilon \ll 1$ limit in the previous section still proved difficult to solve analytically, we considered the simpler case $\mathscr{K} = 0$. This corresponds to the case where the vessel wall is able to open and close, but there is no change in the resistance to the flow associated with this constriction.

As before, we take $p_L = 0$ and use a complex representation. The governing equation (22) becomes

$$\frac{\partial \theta}{\partial \tau} = \mathscr{D} \frac{\partial^2 \theta}{\partial \xi^2}\,, \tag{54}$$

subject to

$$\int_0^1 \theta \,\mathrm{d}x = \mathscr{V}\,. \tag{55}$$

$$\theta(0,\tau) = 1 - \epsilon \mathrm{e}^{\mathrm{i}\tau} - \sigma\,, \tag{56}$$

$$\theta(1,\tau) = -\sigma\,. \tag{57}$$

We employ the same series expansion (34)–(35) as before, and substitute into the system of equations (54)–(57). The leading-order solution is found to be

$$\bar{\theta} = \mathscr{V} + \frac{1}{2} - \xi\,, \tag{58}$$

$$\bar{\sigma} = \frac{1}{2} - \mathscr{V}\,. \tag{59}$$

Hence, the leading-order blood pressure is given by

$$\bar{p} = \bar{\theta} + \bar{\sigma} = 1 - \xi\,. \tag{60}$$

At first order in ϵ, the governing equation for θ' is

$$\mathrm{i}\theta' = \mathscr{D} \frac{\partial^2 \theta'}{\partial \xi^2}\,, \tag{61}$$

and the integral and boundary conditions are

$$\int_0^1 \theta' \,\mathrm{d}x = 0\,, \tag{62}$$

$$\theta'(0) = -1 - \sigma'\,, \tag{63}$$

$$\theta'(1) = -\sigma'\,. \tag{64}$$

The general solution to (61) may be written as

$$\theta'(\xi) = A \sinh\left(\frac{(1+\mathrm{i})}{\sqrt{2\mathscr{D}}}\,\xi\right) + B \sinh\left(\frac{(1+\mathrm{i})}{\sqrt{2\mathscr{D}}}\,(1-\xi)\right)\,. \tag{65}$$

The three conditions (62)–(64) are then trivially applied to obtain

$$A = -B = \left[\sinh\left(\frac{(1+\mathrm{i})}{\sqrt{2\mathscr{D}}}\right)\right]^{-1}\,, \qquad \sigma' = -\frac{1}{2}\,. \tag{66}$$

The physical solutions are obtained by taking the real parts of θ and σ. The complex constants A and B make this quite an involved process for θ, but for σ we simply have

$$\sigma(\tau) = \frac{1}{2} - \mathscr{V} - \tfrac{1}{2}\epsilon \cos\tau + O(\epsilon^2)\,, \tag{67}$$

and we are interested in comparing this with $p(0,\tau)/P^* = 1 - \epsilon\cos\tau$. The cuff pressure variations are therefore in phase with the arterial pressure variations, and have precisely half the amplitude

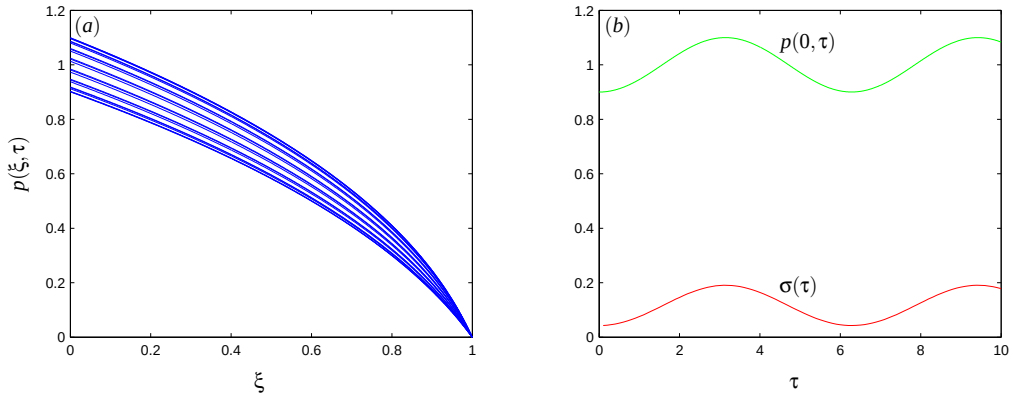

FIGURE 11: *Numerical results for the Finapres model, showing* (a) *the spatial variation of the fluid pressure at various time steps and* (b) *the temporal variation of* σ *(red) and the upstream pressure* $p(0,\tau)$ *(green). Here* $\mathscr{K} = 0.5$, $\mathscr{V} = 0.5$, $\mathscr{D} = 1$, $\epsilon = 0.1$ *and* $p_L = 0$.

of the imposed upstream arterial pressure. Even if $\mathscr{V}$ is chosen carefully, the output σ will need to be calibrated in order to provide a good measurement of the true arterial pressure.

During the calibration produce of the device, σ is held fixed, and the variation of $\mathscr{V}$ is recorded, but (67) still holds. Interestingly, this suggests that the amplitude of variations in $\mathscr{V}$ is independent of the fixed value of σ chosen. While discrepancies will probably arise at $O(\epsilon^2)$, we may well need a better model (quite possibly involving a more accurate tube law, and accounting for the fact that the cuff and finger will separate rather than allowing negative transmural pressures) in order to capture the details of the calibration process.

However, we also have that $\mathscr{V}$ contains a factor of k so, after calibration, any changes in the stiffness of the artery wall will affect the value of $\mathscr{V}$ and hence disrupt the calibration, altering the readings obtained.

3.5 Numerical solutions

We solve the full non-linear governing equations using the backwards Euler method (a first-order implicit finite difference method), using Newton's method to solve the matrix problem at each time step and choosing the steady state derived in section 3.3 as an initial condition.

Numerical solutions for $\mathscr{K} = 0.5$, $\mathscr{V} = 0.5$, and $\mathscr{D} = 1$ are shown in figure 11. The spatial variation of $p(\xi,\tau)$ is confined within a fixed envelope defined by the oscillations in pressure at the upstream end. Correspondingly, the cuff pressure $\sigma(\tau)$ exhibits oscillations of approximately the same frequency and in phase with the oscillations in pressure.

To investigate the influence of varying the stiffness of the arterial walls we increase the dimensional parameter k whilst holding all other parameters fixed. To achieve this using our choice of non-dimensional parameters we increase $\mathscr{K}$ whilst holding the values of $\mathscr{K}\mathscr{D}$ and $\mathscr{V}\mathscr{K}$ constant. The temporal variation of σ for increasing k is shown in figure 12, where we observe that increasing the compliance of the arterial walls serves to increase the mean value of the blood pressure measurement.

Thus, this model indicates that the Finapres blood pressure measurement is sensitive to changes in arterial stiffness in direct contrast to the model for the Colin tonometer.

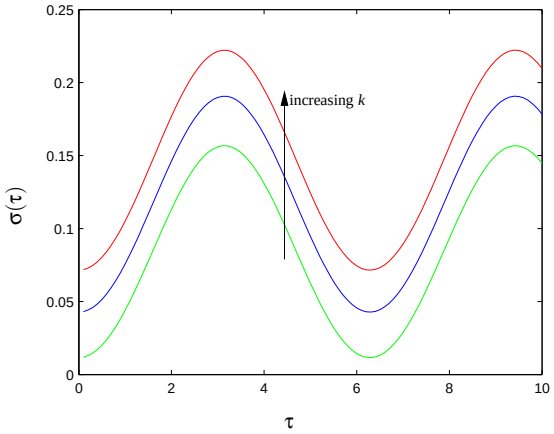

FIGURE 12: *Numerical results for the Finapres model, showing the temporal variation of σ for increasing arterial compliance (k). Here $\mathscr{K} = 0.95$ (green), $\mathscr{K} = 1$ (blue) and $\mathscr{K} = 1.05$ (red) where $\mathscr{K}\mathscr{D} = 0.5$, $\mathscr{V}\mathscr{K} = 0.5$, $\epsilon = 0.1$ and $p_L = 0$.*

4 Discussion and future work

The motivation of this study was the difference observed in measurements of transitional changes in arterial blood pressure by the Finapres and Colin Radial Artery Tonometer. In this report we have developed and solved mathematical models of these two devices both in order to provide insight into the readings they give, and as a first step towards explaining the discrepancies observed, in particular by testing the hypothesis that changes in arterial stiffness may be behind the different results.

Our spring-and-dashpot model for the Tonometer suggests that readings are likely to be insensitive to the elastic properties of the patient's wrist (which are patient-dependent). Since this model is simplistic we also proposed a two-dimensional model of the system. This has yet to be fully solved, but we anticipate that it will describe the behaviour of the tonometer more accurately. If the portion of the artery wall adjacent to the tonometer is held flat, then the tension in the wall, which acts mainly through curvature effects, will be significantly reduced.

For the Finapres, we developed and solved a model of one-dimensional blood flow in the artery under the cuff. In the limit of small-amplitude time-dependent oscillations in the arterial pressure, and furthermore assuming that the vessel resistance does not depend on its radius, we were able to find the first few terms in a series expansion analytically. This solution showed the measured readings are expected to oscillate in phase with the arterial pressure, although their absolute values may differ. Hence a calibration of the cuff pressure should really be performed to yield the arterial pressure. Increasing arterial wall stiffness k^{-1} could affect both the mean cuff pressure and the amplitude of the pressure variations. Preliminary numerical results appear to suggest that higher cuff pressures will be recorded in patients with stiffer arteries. This model does not incorporate the effect of the blood in the vein, so future work could involve developing a similar vein model that can be coupled with the existing model, using an appropriate model of the capillaries. Some possible models were briefly described in the text.

Our preliminary results suggest that provoked sympathetic peripheral vasoconstriction may be able to explain the discrepancies observed, though further investigation is certainly required.

In common with much mathematical modelling work, one major weakness lies in the accurate determination of suitable parameters. In order to facilitate comparison of the two measurements, we discussed developing an additional Tonometer model in which blood flow in the artery is

treated as a one-dimensional flow in a compliant tube, in a similar way to the Finapres model. Aligning the two models in this way means that they would have some parameters in common, enabling a better comparison of the behaviours of the two readings, and hence a better basis on which to investigate the discrepancies.

References

Birch, A. A. 2007 Sympathetic peripheral vasoconstriction may be measured using an artefact of the Finapres volume clamp technique. *Blood Pressure Monit.* **12** (5), 315–319.

Birch, A. A. & Morris, S. L. 2003 Do the Finapres^{TM} and Colin® radial artery tonometer measure the same blood pressure changes following deflation of thigh cuffs? *Physiol. Meas.* **24** (3), 653–660.

Birch, A. A., Neil-Dwyer, G. & Murrills, A. J. 2002 The repeatability of cerebral autoregulation assessment using sinusoidal lower body negative pressure. *Physiol. Meas.* **23** (1), 73–83.

Drzewiecki, G., Solanki, B., J.-J., W. & Li, J. K.-L. 1996 Noninvasive determination of arterial pressure and volume using tonometry. In *Proc. IEEE EMBS Conf.*, pp. 61–64.

Fung, Y. C. 1993 *Biomechanics: Mechanical Properties of Living Tissues*, 2nd edn. Springer–Verlag.

Imholz, B. P. M., Wieling, W., van Montfrans, G. A. & Wesseling, K. H. 1998 Fifteen years experience with finger arterial pressure monitoring: assessment of the technology. *Cardiovasc. Res.* **38** (3), 605–616.

Kemmotsu, O., Ueda, M., Otsuka, H., Yamamura, T., Winter, D. C. & Eckerle, J. S. 1991 Arterial tonometry for noninvasive, continuous blood-pressure monitoring during anesthesia. *Anesthesiology* **75** (2), 333–340.

Langewouters, G. J., Zwart, A., Busse, R. & Wesseling, K. H. 1986 Pressure diameter relationships of segments of human finger arteries. *Clin. Phys. Physiol. Meas.* **7** (1), 43–56.

O'Brien, E., Waeber, B., Parati, G., Staessen, J. & Myers, M. G. 2001 Blood pressure measuring devices: recommendations of the european society of hypertension. *British Medical Journal* **322** (7285), 531–536.

Penaz, J. 1973 Photoelectric measurement of blood pressure, volume and flow in the finger. In *Digest 10th International Conference on Medical and Biological Engineering*, p. 104. Dresden.

Sato, T., Nishinaga, M., Kawamoto, A., Ozawa, T. & Takatsuji, H. 1993 Accuracy of a continuous blood-pressure monitor based on arterial tonometry. *Hypertension* **21** (6), 866–874.

Weiss, B. M., Spahn, D. R., Rahmig, H., Rohling, R. & Pasch, T. 1996 Radial artery tonometry: Moderately accurate but unpredictable technique of continuous non-invasive arterial pressure measurement. *Brit. J. Anaeth.* **76** (3), 405–411.

Wesseling, K. H., Dewit, B., Vanderhoeven, G. M. A., Vangoudoever, J. & Settels, J. J. 1995 Physiocal: Calibrating finger vascular physiology for Finapres. *Homeost. Health Desease* **36** (2-3), 67–82.